# Co-ordination Chemistry of Higher Oxidation States. Part 40.[1] Spectroscopic, Electrochemical and Structural Studies of Cationic Osmium-(III) and -(IV) Diphosphine and Diarsine Complexes†

**Neil R. Champness,[a] William Levason,*[,a] Derek Pletcher,[a] Mark D. Spicer[b] and Michael Webster[a]**
[a] *Department of Chemistry, University of Southampton, Southampton SO9 5NH, UK*
[b] *Department of Pure and Applied Chemistry, University of Strathclyde, Glasgow G1 1XL, UK*

The osmium(III) complexes *trans*-$[Os(L{-}L)_2X_2]BF_4$ [X = Cl or Br; L–L = *o*-$C_6H_4(PMe_2)_2$, *o*-$C_6H_4(AsMe_2)_2$, *o*-$C_6H_4(AsMe_2)(PMe_2)$, *o*-$C_6F_4(AsMe_2)_2$, $Ph_2PCH_2CH_2PPh_2$, $Me_2PCH_2CH_2PMe_2$, $Ph_2AsCH{=}CHAsPh_2$, *o*-$C_6H_4(PPh_2)_2$ or *o*-$C_6F_4(PPh_2)_2$] have been prepared by dilute $HNO_3$ oxidation of the osmium(II) analogues in aqueous $HBF_4$. Concentrated $HNO_3$ converts most of these complexes into $Os^{IV}$, but the unstable *trans*-$[Os(L{-}L)_2X_2][ClO_4]_2$ were isolated as solids only for L–L = *o*-$C_6H_4(PMe_2)_2$, *o*-$C_6H_4(AsMe_2)_2$ or *o*-$C_6H_4(AsMe_2)(PMe_2)$. Cyclic voltammetry reveals that the $Os^{II}$–$Os^{III}$ and $Os^{III}$–$Os^{IV}$ couples are generally reversible. Assignments of the UV/VIS spectra of the osmium-(III) and -(IV) complexes are proposed. The X-ray structure of *trans*-$[Os\{o\text{-}C_6H_4(AsMe_2)_2\}_2Cl_2]ClO_4$ is reported: monoclinic, space group *C*2/*m*, *a* = 13.890(2), *b* = 10.381(2), *c* = 11.682(3) Å, β = 113.86(2)°, *Z* = 2, and with *R* = 0.039. Osmium $L_{III}$-edge (and where appropriate bromine K-edge) extended X-ray absorption fine structure data for the complexes *trans*-$[Os\{o\text{-}C_6H_4(AsMe_2)_2\}_2X_2]^{n+}$ (*n* = 0–2) are reported and the trends in Os–As and Os–X bond lengths with changing osmium oxidation state are discussed.

In recent studies[2–4] we have shown that stepwise replacement of halides (X = Cl or Br) by neutral ligands (L = $PR_3$, $AsR_3$, $SbR_3$, *etc.*) in the anions $[OsX_6]^{2-}$ makes the osmium(IV) complexes progressively more strongly oxidising, as evidenced by the increasingly positive $Os^{III}$–$Os^{IV}$ redox potentials. The $[OsL_4X_2]^{2+}$ complexes were formed only in concentrated $HNO_3$ solution and with a limited range of ligands,[4] and solid complexes were not isolated due to their high solubility in the acid. Increased stability is expected to result from replacement of the monodentate L by the corresponding bidentate ligands. However, although osmium(II) complexes $[Os(L{-}L)_2X_2]$ (L–L = diphosphine or diarsine) have been thoroughly studied,[5–9] little is known about the osmium(III) analogues, and osmium(IV) complexes have been isolated only with *o*-$C_6H_4(AsMe_2)_2$.[5] For the complexes of $Os^{III}$ or $Os^{IV}$ there are little spectroscopic data and no structural characterisation. Here we report detailed studies of a range of such complexes.

## Experimental

Physical measurements were made as described previously,[4] except that UV/VIS spectra were obtained using a Perkin-Elmer Lambda 19 spectrometer.

*Osmium*(III) *Complexes*.—The osmium starting materials were made as described previously.[2–4] Syntheses of osmium complexes with methyl-substituted ligands were carried out under a nitrogen atmosphere. The crude osmium(II) complexes were prepared by three separate methods, the preferred method being from 2-methoxyethanol solution. Osmium(III) complexes were prepared from the crude osmium(II) species.

*trans*-$[Os\{o\text{-}C_6H_4(PMe_2)_2\}_2Cl_2]BF_4$. To a deoxygenated solution of $[NH_4]_2[OsCl_6]$ (0.27 g, 0.63 mmol) in 2-methoxyethanol (30 cm$^3$) and water (3 cm$^3$) was added *o*-$C_6H_4(PMe_2)_2$ (0.40 g, 2.0 mmol) *via* a syringe. The mixture was refluxed for 2 h with stirring. Upon cooling a yellow solid was deposited from the red solution. It was filtered off, washed with diethyl ether and dried *in vacuo*. The osmium(III) complex was then prepared by adding concentrated $HNO_3$ dropwise (1 cm$^3$ in total) to the crude osmium(II) species suspended in 40% $HBF_4$ (15 cm$^3$). The mixture was then stirred for 10 min, the purple solid filtered off, washed with water and then diethyl ether, and dried *in vacuo* (0.15 g, 32%) (Found: C, 32.4; H, 4.4. $C_{20}H_{32}BCl_2F_4OsP_4$ requires C, 32.3; H, 4.3%).

The following complexes were prepared analogously: *trans*-$[Os\{o\text{-}C_6F_4(PPh_2)_2\}_2Cl_2]BF_4$ (37%) (Found: C, 52.2; H, 2.5. $C_{60}H_{40}BCl_2F_{12}OsP_4$ requires C, 52.0; H, 2.9%), $\Lambda_m$(MeCN) = 140 $\Omega^{-1}$ cm$^2$ mol$^{-1}$; *trans*-$[Os\{o\text{-}C_6H_4(AsMe_2)(PMe_2)\}_2Cl_2]BF_4$ (33%) (Found: C, 29.5; H, 3.7. $C_{20}H_{32}As_2BCl_2F_4OsP_2$ requires C, 28.9; H, 3.9%), $\Lambda_m$(MeCN) = 142 $\Omega^{-1}$ cm$^2$ mol$^{-1}$; *trans*-$[Os(Ph_2AsCH{=}CHAsPh_2)_2Cl_2]BF_4$ (35%) (Found: C, 47.0; H, 3.2. $C_{52}H_{44}As_4BCl_2F_4Os$ requires C, 47.4; H, 3.4%).

The following complexes were prepared similarly, but using $K_2[OsBr_6]$ as the starting material: *trans*-$[Os(Me_2PCH_2CH_2PMe_2)_2Br_2]BF_4$ (29%) (Found: C, 19.3; H, 4.3. $C_{12}H_{32}BBr_2F_4OsP_4$ requires C, 19.5; H, 4.4%); *trans*-$[Os\{o\text{-}C_6H_4(PMe_2)_2\}_2Br_2]BF_4$ (30%) (Found: 28.4; H, 3.7. $C_{20}H_{32}BBr_2F_4OsP_4$ requires C, 28.8; H, 3.9%); *trans*-$[Os\{o\text{-}C_6H_4(PPh_2)_2\}_2Br_2]BF_4$ (24%), $\Lambda_m$(MeCN) = 161 $\Omega^{-1}$ cm$^2$ mol$^{-1}$ (Found: C, 54.4; H, 3.7. $C_{60}H_{48}BBr_2F_4OsP_4$ requires C, 54.2; H, 3.6%); *trans*-$[Os\{o\text{-}C_6H_4(AsMe_2)(PMe_2)\}_2Br_2]BF_4$ (35%) (Found: C, 25.8; H, 3.4. $C_{20}H_{32}As_2BBr_2F_4OsP_2$ requires C, 26.1; H, 3.5%); *trans*-$[Os(Ph_2AsCH{=}CHAsPh_2)_2Br_2]BF_4$, impure initially, purified by refluxing in ethanol (30 cm$^3$) and 40% $HBF_4$ (10 cm$^3$) for 1 h (21%) (Found: C, 44.2; H, 3.0. $C_{52}H_{44}As_4BBr_2F_4Os$ requires C, 44.4; H, 3.1%).

The following complexes were made as for *trans*-$[Os\{o\text{-}C_6H_4(PMe_2)_2\}_2Cl_2]BF_4$ using ethanol in place of 2-methoxyethanol; *trans*-$[Os\{o\text{-}C_6H_4(AsMe_2)_2\}_2Cl_2]BF_4$ (13%) (Found:

---

† *Supplementary data available:* see Instructions for Authors, *J. Chem. Soc., Dalton Trans.*, 1992, Issue 1, pp. xx–xxv.

*Non-SI unit employed:* eV ≈ 1.60 × $10^{-19}$ J.

**Table 1** Atomic coordinates for *trans*-$[Os\{o\text{-}C_6H_4(AsMe_2)_2\}_2Cl_2]ClO_4$

| Atom | $x$ | $y$ | $z$ |
|---|---|---|---|
| Os | 0.0000 | 0.0000 | 0.0000 |
| As(1) | 0.2051(1) | 0.0000 | 0.0529(1) |
| As(2) | −0.0183(1) | 0.0000 | −0.2179(1) |
| Cl(1) | 0.0000 | 0.2251(3) | 0.0000 |
| C(1) | 0.2940(7) | 0.1462(9) | 0.1451(8) |
| C(2) | 0.2259(9) | 0.0000 | −0.1052(11) |
| C(3) | 0.3362(10) | 0.0000 | −0.1002(11) |
| C(4) | 0.3497(11) | 0.0000 | −0.2110(13) |
| C(5) | 0.2580(12) | 0.0000 | −0.3247(15) |
| C(6) | 0.1500(12) | 0.0000 | −0.3256(13) |
| C(7) | 0.1347(10) | 0.0000 | −0.2138(11) |
| C(8) | −0.0910(8) | 0.1473(10) | −0.3239(9) |
| Cl(2) | 0.5000 | 0.0000 | 0.5000 |
| O(1)* | 0.5026(19) | 0.0000 | 0.3898(23) |
| O(2)* | 0.6314(49) | 0.0000 | 0.5567(53) |
| O(3)* | 0.5000 | 0.1429(47) | 0.5000 |

* Common refined isotropic thermal parameter and refined site populations [O(1) 0.48(3), O(2) 0.24(2), O(3) 0.29(2)].

C, 25.9; H, 3.5. $C_{20}H_{32}As_4BCl_2F_4Os$ requires C, 26.1; H, 3.5%); *trans*-$[Os(Ph_2PCH_2CH_2PPh_2)_2Cl_2]BF_4$ (21%) (Found: C, 54.5; H, 4.2. $C_{52}H_{48}BCl_2F_4OsP_4$ requires C, 54.6; H, 4.2%); *trans*-$[Os(Me_2PCH_2CH_2PMe_2)_2Cl_2]BF_4$ (16%) (Found: C, 22.0; H, 5.1. $C_{12}H_{32}BCl_2F_4OsP_4$ requires C, 22.2; H, 5.0%); *trans*-$[Os\{o\text{-}C_6H_4(AsMe_2)_2\}_2Br_2]BF_4$, from $K_2[OsBr_6]$ (26%) (Found: C, 23.9; H, 3.2. $C_{20}H_{32}As_4BBr_2F_4Os$ requires C, 23.8; H, 3.2%).

*trans*-$[Os\{o\text{-}C_6F_4(AsMe_2)_2\}_2Cl_2]BF_4$. A deoxygenated ethanol (35 cm$^3$) solution of $OsO_4$ (0.08 g, 0.3 mmol) and concentrated HCl (3 cm$^3$) was brought to reflux and to this solution $o\text{-}C_6F_4(AsMe_2)_2$ (0.49 g, 1.4 mmol) was added. The mixture was refluxed for 2 h and upon cooling a yellow solid was precipitated. It was filtered off, washed with diethyl ether, dried *in vacuo*, then suspended in 40% $HBF_4$ (15 cm$^3$) and oxidised by dropwise addition of concentrated $HNO_3$ (1 cm$^3$). The pink solid was filtered off, washed with water and then with diethyl ether, and dried *in vacuo* (0.04 g, 14%) (Found: C, 23.0; H, 2.5. $C_{20}H_{24}As_4BCl_2F_{12}Os$ requires C, 22.6; H, 2.3%), $\Lambda_m$(MeCN) = 144 $\Omega^{-1}$ cm$^2$ mol$^{-1}$.

The complex *trans*-$[Os\{o\text{-}C_6H_4(PPh_2)_2\}_2Cl_2]BF_4$ was prepared analogously (41%) (Found: C, 57.9; H, 3.9. $C_{60}H_{48}BCl_2F_4OsP_4$ requires C, 58.1; H, 3.9%).

The following complexes were prepared similarly, replacing concentrated HCl with concentrated HBr: *trans*-$[Os(Ph_2PCH_2CH_2PPh_2)_2Br_2]BF_4$ (45%) (Found: C, 50.5; H, 4.0. $C_{52}H_{48}BBr_2F_4OsP_4$ requires C, 50.6; H, 3.9%), $\Lambda_m$(MeCN) = 142 $\Omega^{-1}$ cm$^2$ mol$^{-1}$; *trans*-$[Os\{o\text{-}C_6F_4(PPh_2)_2\}_2Br_2]BF_4$, impure initially, purified by refluxing the crude product in ethanol (30 cm$^3$) and 40% $HBF_4$ (10 cm$^3$) for 1 h (31%) (Found: C, 48.7; H, 3.0. $C_{60}H_{40}BBr_2F_{12}OsP_4$ requires C, 48.9; H, 2.7%); *trans*-$[Os\{o\text{-}C_6F_4(AsMe_2)_2\}_2Br_2]BF_4$ (19%) (Found: C, 20.5; H, 2.0. $C_{20}H_{24}As_4BBr_2F_{12}Os$ requires C, 20.8; H, 2.1%).

*Osmium*(IV) *Complexes General Method.* **CAUTION**: Perchlorate complexes are unpredictably explosive, and should be prepared in small quantities and with due precautions.

The finely powdered osmium(III) complex (*ca.* 0.3 mmol) was cooled to *ca.* −5 °C, and concentrated $HNO_3$ added dropwise with stirring until the solid just dissolved. Concentrated perchloric acid (70%, 1 cm$^3$) was added, and the mixture maintained at *ca.* −5 °C until the solid complex had separated. The solid was compacted by centrifuging, the supernatant liquid removed, and the solid washed with dry diethyl ether (5 cm$^3$) and dried *in vacuo*. Some samples were also isolated by filtration and washed with diethyl ether. Yields 60–70%.

*trans*-$[Os\{o\text{-}C_6H_4(AsMe_2)_2\}_2Cl_2][ClO_4]_2$ (Found: C, 23.4; H, 3.0. $C_{20}H_{32}As_4Cl_4O_8Os$ requires C, 23.3; H, 3.1%); *trans*-$[Os\{o\text{-}C_6H_4(AsMe_2)_2\}_2Br_2][ClO_4]_2$ (Found: C, 21.5; H, 3.0. $C_{20}H_{32}As_4Br_2Cl_2O_8Os$ requires C, 21.4; H, 2.8%), ν(Os–Br) 250 cm$^{-1}$; *trans*-$[Os\{o\text{-}C_6H_4(AsMe_2)(PMe_2)\}_2Cl_2][ClO_4]_2$ (Found: C, 25.6; H, 3.5. $C_{20}H_{32}As_2Cl_4O_8OsP_2$ requires C, 25.6; H, 3.4%); *trans*-$[Os\{o\text{-}C_6H_4(AsMe_2)(PMe_2)\}_2Br_2][ClO_4]_2$ (Found: C, 23.0; H, 3.0. $C_{20}H_{32}As_2Br_2Cl_2O_8OsP_2$ requires C, 23.25; H, 3.1%), ν(Os–Br) 249 cm$^{-1}$; *trans*-$[Os\{o\text{-}C_6H_4(PMe_2)_2\}_2Cl_2][ClO_4]_2$ (Found: C, 28.4; H, 4.1. $C_{20}H_{32}Cl_4O_8OsP_4$ requires C, 28.1; H, 3.8%); *trans*-$[Os\{o\text{-}C_6H_4(PMe_2)_2\}_2Br_2][ClO_4]_2$ (Found: C, 25.6; H, 3.6. $C_{20}H_{32}Br_2Cl_2O_8OsP_4$ requires C, 25.4; H, 3.4%).

*Crystallography*.—Dark red air-stable rhomb-shaped crystals of $[Os\{o\text{-}C_6H_4(AsMe_2)_2\}_2Cl_2]ClO_4$ were obtained by vapour diffusion of $Et_2O$ into MeCN solutions and mounted in thin-walled glass capillaries. Preliminary photographic X-ray examination established approximate cell dimensions and the crystal quality. The density was measured by flotation ($CCl_4$–$C_2H_4Br_2$).

*Crystal data*. $C_{20}H_{32}As_4Cl_3O_4Os$, $M = 932.7$, monoclinic, space group $C2/m$, $a = 13.890(2)$, $b = 10.381(2)$, $c = 11.682(3)$ Å, $\beta = 113.86(2)°$, $U = 1429.6$ Å$^3$, $D_m = 2.18(2)$, $Z = 2$, $D_c = 2.166$ g cm$^{-3}$, $F(000) = 886$, $\lambda$(Mo-K$\alpha$) = 0.710 69 Å, $\mu = 93.2$ cm$^{-1}$.

Data were collected on an Enraf-Nonius CAD4 diffractometer using graphite-monochromated molybdenum radiation and a room-temperature crystal (0.38 × 0.35 × 0.02 mm). Cell dimensions were determined from 25 reflections and 1450 reflections were recorded ($1.5 < \theta < 25°$; $h$ −15 to 15, $k$ 0–12, $l$ 0–13). The three check reflections showed no significant change during the experiment and an empirical $\psi$-scan absorption correction based on three reflections was applied along with the usual Lorentz and polarisation corrections (transmission: minimum 29.8; maximum 99.9%). After data reduction there were 1340 unique reflections ($R_{int} = 0.013$) and those (1168) with $F > 3\sigma(F)$ were used in the structure refinement. The systematic absences ($hkl$, $h + k = 2n$; $0k0$, $k = 2n$) established that the space group was $C2$, $Cm$ or $C2/m$. With $Z = 2$, the Os and Cl (of $ClO_4^-$) must be located on special positions and perchlorate disorder can be absent only in the (non-centrosymmetric) $C2$ or $Cm$. The average value of $|E^2 - 1|$ was in the region appropriate for non-centrosymmetric space groups, although with heavy-atom structures this can be misleading.[10] The trial structure containing Os, As and Cl (cation) was developed by inspection of the Patterson synthesis in the space group $C2$. Subsequent structure-factor and electron-density syntheses revealed the C, Cl (anion) and O atoms. The geometry of the perchlorate anion was not satisfactory with unusual Cl anisotropic thermal parameters and bond angles. In addition the highest peaks in the difference electron-density map were potential O atoms of a disordered anion. Although the data refined to $R = 0.04$ the least-squares refinement did not converge satisfactorily. Inspection of the atomic coordinates of the cation showed that this part of the molecule was very close to $2/m$ symmetry which the space group $C2/m$ would require and that since there was convincing evidence for perchlorate disorder the structure was examined in this space group. The refinement proceeded smoothly to convergence and the introduction of anisotropic C atoms posed no problem (unlike $C2$) and subsequent analysis was continued in this space group. The perchlorate O atoms were given a common refined isotropic thermal parameter and refined populations which accounted for four O atoms per residue. No H atoms were included in the model. Full-matrix least-squares refinement on $F$ converged to $R = 0.039$ {89 parameters, 1168 reflections, anisotropic (Os, As, Cl, C) and isotropic (O) atoms, $w^{-1} = [\sigma^2(F) + 0.0005F^2]$, $R' = 0.056$, maximum shift/error = 0.08} with the residual electron density in the range +1.17 to −1.90 e Å$^{-3}$. The final atomic coordinates are given in Table 1. Scattering factors for neutral atoms and anomalous dispersion corrections

**Table 2** Selected spectroscopic data on the osmium(III) complexes

| Compound | Colour | ν(Os–X)$^a$/cm$^{-1}$ | $E_{max}$$^b$/10$^3$ cm$^{-1}$ (ε/dm$^3$ mol$^{-1}$ cm$^{-1}$) |
|---|---|---|---|
| $[Os(Ph_2PCH_2CH_2PPh_2)_2Cl_2]BF_4$ | Dark green | 320 | 16.7 (1300), 23.6 (860), 31.2 (890) |
| $[Os(Me_2PCH_2CH_2PMe_2)_2Cl_2]BF_4$ | Purple | 316 | 17.8 (875), 20.4 (170), 30.1 (1075) |
| $[Os\{o\text{-}C_6H_4(PMe_2)_2\}_2Cl_2]BF_4$ | Purple | 316 | 18.1 (2370), 21.0 (400), 29.8 (2400) |
| $[Os\{o\text{-}C_6H_4(PPh_2)_2\}_2Cl_2]BF_4$ | Green | 330 | 16.2 (1000), 19.3 (490), 23.2 (890), 29.2 (sh) |
| $[Os\{o\text{-}C_6F_4(PPh_2)_2\}_2Cl_2]BF_4$ | Green | 331 | 16.0 (1370), 22.6 (1280), 28.9 (1090) |
| $[Os\{o\text{-}C_6H_4(AsMe_2)(PMe_2)\}_2Cl_2]BF_4$ | Mauve | 325 | 18.6 (1960), 21.2 (480), 30.6 (1950) |
| $[Os\{o\text{-}C_6H_4(AsMe_2)_2\}_2Cl_2]BF_4$ | Mauve | 325 | 18.8 (2280), 21.3 (610), 30.8 (2130) |
| $[Os\{o\text{-}C_6F_4(AsMe_2)_2\}_2Cl_2]BF_4$ | Pink | 324 | 19.2 (1060), 21.2 (300), 30.1 (770) |
| $[Os(Ph_2AsCH{=}CHAsPh_2)_2Cl_2]BF_4$ | Purple | 330 | 17.4 (1910), 20.1 (780), 24.4 (1255), 30.0 (1270) |
| $[Os(Ph_2PCH_2CH_2PPh_2)_2Br_2]BF_4$ | Dark green | n.o. | 15.7 (3570), 17.7 (sh), 20.6 (650), 26.9 (820) |
| $[Os(Me_2PCH_2CH_2PMe_2)_2Br_2]BF_4$ | Light blue | n.o. | 16.3 (1570), 18.2 (sh), 25.9 (710) |
| $[Os\{o\text{-}C_6H_4(PMe_2)_2\}_2Br_2]BF_4$ | Blue | n.o. | 16.4 (3570), 18.8 (570), 25.6 (1270) |
| $[Os\{o\text{-}C_6H_4(PPh_2)_2\}_2Br_2]BF_4$ | Dark blue | 225 | 15.3 (4530), 18.0 (1430), 19.6 (sh), 26.9 (1120) |
| $[Os\{o\text{-}C_6F_4(PPh_2)_2\}_2Br_2]BF_4$ | Blue | 240 | 16.5 (1440), 19.9 (1250), 26.2 (1520) |
| $[Os\{o\text{-}C_6H_4(AsMe_2)(PMe_2)\}_2Br_2]BF_4$ | Blue | 234 | 16.9 (6280), 19.0 (850), 26.8 (1900) |
| $[Os\{o\text{-}C_6H_4(AsMe_2)_2\}_2Br_2]BF_4$ | Blue | 247 | 17.0 (5950), 19.2 (1950), 21.7 (30), 27.2 (2150) |
| $[Os\{o\text{-}C_6F_4(AsMe_2)_2\}_2Br_2]BF_4$ | Blue | n.o. | 17.1 (1810), 19.0 (250), 26.5 (410) |
| $[Os(Ph_2AsCH{=}CHAsPh_2)_2Br_2]BF_4$ | Blue | 237 | 16.0 (5910), 18.3 (1440), 21.5 (1110), 26.5 (1380) |

$^a$ Nujol mull, n.o. = not observed or assigned. $^b$ In $CH_2Cl_2$ solution.

**Table 3** Bond lengths (Å) and angles (°) for *trans*-$[Os\{o\text{-}C_6H_4(AsMe_2)_2\}_2Cl_2]ClO_4$

| | | | |
|---|---|---|---|
| Os–Cl(1) | 2.337(3) | As(1)–C(1) | 1.944(8) |
| Os–As(1) | 2.459(1) | As(1)–C(2) | 1.971(12) |
| Os–As(2) | 2.459(1) | As(2)–C(7) | 1.953(11) |
| | | As(2)–C(8) | 1.952(9) |
| C–C | minimum 1.34(2) | maximum 1.40(2) | |
| Cl(2)–O | minimum 1.30(2) | maximum 1.55(4) | |
| As(1) • • • As(2) | 3.305(1) | As • • • Cl(1) | 3.393(2) |
| As(1)–Os–As(2) | 84.5(1) | | |
| Os–As(1)–C(1) | 118.2(2) | Os–As(2)–C(8) | 118.5(3) |
| Os–As(1)–C(2) | 107.7(3) | Os–As(2)–C(7) | 107.5(4) |
| C–As–C | minimum 102.6(4) | maximum 104.2(3) | |
| As–C–C | minimum 118.8(9) | maximum 121.1(9) | |
| C–C–C | minimum 118.3(12) | maximum 122.0(11) | |

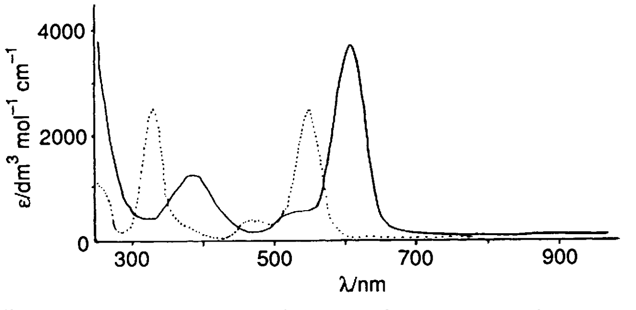

Fig. 1 The UV/VIS spectra of *trans*-$[Os\{o\text{-}C_6H_4(PMe_2)_2\}_2Cl_2]BF_4$ (· · ·) and *trans*-$[Os\{o\text{-}C_6H_4(PMe_2)_2\}_2Br_2]BF_4$ (——) in $CH_2Cl_2$

were taken from SHELX 76[11] (Cl, O, C) and ref. 12 (Os, As). All calculations were performed using SHELX 76,[11] XANADU[13] and ORTEP II[14] on an IBM 3090 computer.

Additional material available from the Cambridge Crystallographic Data Centre comprises thermal parameters and remaining bond lengths and angles.

*Extended X-Ray Absorption Fine Structure* (*EXAFS*).—The X-ray absorption spectra were recorded in transmission mode at the Daresbury Synchrotron Radiation Source operating at 2 GeV and an average beam current of *ca.* 150 mA. Osmium $L_{III}$-edge data were collected on station 7.1 using a Si(111) order-sorting monochromator and bromine K-edge data on station 9.2 using a Si(220) double-crystal monochromator. The room-temperature samples were carefully ground powders diluted with dry boron nitride sealed in 1 mm pathlength holders with Sellotape. Data treatment utilised the programs PAXAS[15] and EXCURVE 90[16] and was carried out as described elsewhere.[17] The compound *trans*-$[Os\{o\text{-}C_6H_4(AsMe_2)_2\}_2Cl_2]ClO_4$ was used as a model to assess the reliability of phase shifts in these systems.

## Results and Discussion

*Osmium*(III) *Complexes*.—The osmium(II) complexes *trans*-$[Os(L\text{–}L)_2X_2]$ were obtained by literature methods[5–7] which involve reaction of $OsO_4$/HX or $[OsX_6]^{2-}$ with L–L in alcohols. The corresponding osmium(III) complexes *trans*-$[Os(L\text{–}L)_2X_2]BF_4$ were prepared by oxidation of the powdered osmium(II) complexes suspended in 40% $HBF_4$ with concentrated $HNO_3$. The isolated complexes and selected spectroscopic data are listed in Table 2. The solid complexes are deeply coloured, air-stable, and easily soluble in a wide range of organic solvents, to give stable solutions in which they are 1:1 electrolytes. They are paramagnetic, μ *ca.* 1.9,[5] and like other osmium(III) complexes exhibit no $^{31}P$ NMR resonances. However the *trans* stereochemistry follows from the presence of a single IR-active ν(Os–X) vibration (Table 2), and from the generally similar UV/VIS spectra to those of *trans*-$[Os(PMe_3)_4Cl_2]BF_4$[4] and *trans*-$[Os\{o\text{-}C_6H_4(AsMe_2)_2\}_2Cl_2]ClO_4$ for which X-ray studies have confirmed the geometry.

Comparison of the UV/VIS spectra with those of *trans*-$[OsL_2X_4]^-$ and *mer*-$[OsL_3X_3]$[2,3] indicates that the major features expected are σ(L)→(Os) and π(X)→(Os) charge-transfer (c.t.) transitions, and the assignments of the spectra of the *trans*-$[Os(L\text{–}L)_2X_2]^+$ cations (Table 2, Fig. 1) are based upon the optical electronegativity approach. The osmium centre has local $D_{4h}$ symmetry and the configuration $(d_{xy})^2,(d_{xz},d_{yz})^3,(d_{z^2})^0,(d_{x^2-y^2})^0(b_2{}^2,e^3,a_1{}^0,b_1{}^0)$. The strong features at 16 000–19 000 cm$^{-1}$ for all complexes are undoubtedly σ(P,As)→e(Os), whilst the major features at *ca.* 30 000 (chlorides) and *ca.* 26 000 cm$^{-1}$ (bromides) are of the appropriate energy[2,3,18–21] to be assigned as the π(X)→e(Os) transitions. However, recognising that the spectra of both series have very similar profiles, with all the bands shifted to lower energy by *ca.* 2000–3000 cm$^{-1}$ between the chlorides and bromides, suggests an alternative assignment for these bands as σ(P,As)→$a_1$(Os). The latter assignment parallels that proposed for some iron(III) analogues,[18] and is consistent with the phosphorus or arsenic charge transfer dominating the spectra when the P(As):X ratio is high. On this basis the weaker π(X)→e(Os) bands lie under the second features and are not resolved.

Table 4 Electrochemical data, $E_e°$/V *vs.* saturated calomel electrode (SCE)*

| Compound | $Os^{II}$–$Os^{III}$ | $Os^{III}$–$Os^{IV}$ |
|---|---|---|
| $[Os(Ph_2PCH_2CH_2PPh_2)_2Cl_2]BF_4$ | 0.28 | 1.48 |
| $[Os(Me_2PCH_2CH_2PMe_2)_2Cl_2]BF_4$ | 0.04 | 1.31 |
| $[Os\{o\text{-}C_6H_4(PMe_2)_2\}_2Cl_2]BF_4$ | 0.24 | 1.49 |
| $[Os\{o\text{-}C_6H_4(PPh_2)_2\}_2Cl_2]BF_4$ | 0.32 | 1.49 |
| $[Os\{o\text{-}C_6F_4(PPh_2)_2\}_2Cl_2]BF_4$ | 0.56 | 1.73 |
| $[Os\{o\text{-}C_6H_4(AsMe_2)(PMe_2)\}_2Cl_2]BF_4$ | 0.15 | 1.43 |
| $[Os\{o\text{-}C_6H_4(AsMe_2)_2\}_2Cl_2]BF_4$ | 0.12 | 1.41 |
| $[Os\{o\text{-}C_6F_4(AsMe_2)_2\}_2Cl_2]BF_4$ | 0.39 | 1.62 |
| $[Os(Ph_2AsCH{=}CHAsPh_2)_2Cl_2]BF_4$ | 0.32 | 1.56 |
| $[Os(Ph_2PCH_2CH_2PPh_2)_2Br_2]BF_4$ | 0.31 | 1.38 |
| $[Os(Me_2PCH_2CH_2PMe_2)_2Br_2]BF_4$ | 0.13 | 1.31 |
| $[Os\{o\text{-}C_6H_4(PMe_2)_2\}_2Br_2]BF_4$ | 0.28 | 1.45 |
| $[Os\{o\text{-}C_6H_4(PPh_2)_2\}_2Br_2]BF_4$ | 0.35 | 1.41 |
| $[Os\{o\text{-}C_6F_4(PPh_2)_2\}_2Br_2]BF_4$ | 0.36 | 1.46 |
| $[Os\{o\text{-}C_6H_4(AsMe_2)(PMe_2)\}_2Br_2]BF_4$ | 0.23 | 1.41 |
| $[Os\{o\text{-}C_6H_4(AsMe_2)_2\}_2Br_2]BF_4$ | 0.18 | 1.37 |
| $[Os\{o\text{-}C_6F_4(AsMe_2)_2\}_2Br_2]BF_4$ | 0.47 | 1.60 |
| $[Os(Ph_2AsCH{=}CHAsPh_2)_2Br_2]BF_4$ | 0.36 | 1.50 |

* In MeCN solution containing 0.1 mol $dm^{-3}$ $NBu^n_4BF_4$. The $[Fe(\eta\text{-}C_5H_5)_2]$–$[Fe(\eta\text{-}C_5H_5)_2]^+$ couple is at 0.41 V.

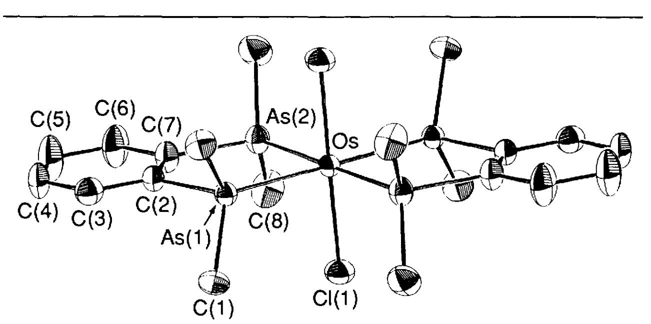

Fig. 2 View of the cation in *trans*-$[Os\{o\text{-}C_6H_4(AsMe_2)_2\}_2Cl_2]ClO_4$ showing the atom numbering scheme. Thermal ellipsoids are drawn with surfaces at the 50% probability level

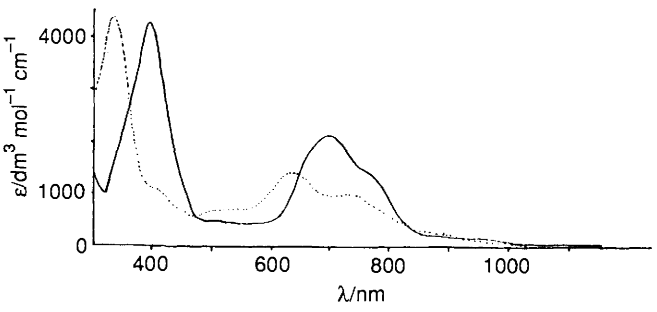

Fig. 3 The UV/VIS spectra of *trans*-$[Os\{o\text{-}C_6H_4(AsMe_2)(PMe_2)\}_2Cl_2][ClO_4]_2$ (· · · ·) and *trans*-$[Os\{o\text{-}C_6H_4(AsMe_2)(PMe_2)\}_2Br_2][ClO_4]_2$ (——) in $CF_3CO_2H$

*Structure of trans*-$[Os\{o\text{-}C_6H_4(AsMe_2)_2\}_2Cl_2]ClO_4$.—The structure consists of discrete *trans*-octahedral cations and heavily disordered perchlorate anions. The cation has 2/*m* crystallographic symmetry and thus the Os, As and the phenyl C atoms are required to be coplanar (see Fig. 2 and Table 3). Several structures containing the bidentate arsine ligand are known and the ligand geometry is unexceptional in the present example. However in the *trans* bis complexes the ligand rings often form a stepped arrangement.[21,22] The Os–Cl(1) distance may be compared with the value[4] of 2.352(4) Å in *trans*-$[Os(PMe_3)_4Cl_2]^+$. A comparison of the bond-length changes with changing osmium oxidation state is presented below.

*Electrochemistry*.—Cyclic voltammetry was used to determine the formal potentials of the $Os^{II}$–$Os^{III}$ and $Os^{III}$–$Os^{IV}$ couples. Voltammograms were recorded at potential scan rates over the range 0.05–0.2 V $s^{-1}$, at a polished, vitreous carbon-disc electrode for $0.5 \times 10^{-3}$ mol $dm^{-3}$ solutions of the osmium(III) complexes in MeCN, containing 0.1 mol $dm^{-3}$ $NBu^n_4BF_4$. The results are listed in Table 4.

The complexes gave reversible $Os^{II}$–$Os^{III}$ and $Os^{III}$–$Os^{IV}$ couples, except for *trans*-$[Os\{o\text{-}C_6H_4(PPh_2)_2\}_2Br_2]BF_4$ which gave an irreversible $Os^{II}$–$Os^{III}$ couple but this is almost certainly due to the insolubility of the osmium(II) complex in acetonitrile. Reversible $Os^{II}$–$Os^{III}$ couples were seen over a range of 0.0–0.6 V while $Os^{III}$–$Os^{IV}$ couples lay between 1.3 and 1.75 V. It can be seen from the data in Table 4 that varying the halide has little effect upon the redox potentials. However, as previously observed,[2–4] replacing alkyl substituents, on the donor atom, with phenyl groups shifts both the $Os^{II}$–$Os^{III}$ and $Os^{III}$–$Os^{IV}$ couples to more positive potentials, and this appears to have a much greater effect than varying the donor atom from P to As. On replacing the *o*-$C_6H_4$ backbone with *o*-$C_6F_4$ the $Os^{II}$–$Os^{III}$ and $Os^{III}$–$Os^{IV}$ potentials were shifted to more positive potentials, as previously observed for the iron and nickel analogues.[23,24] The complex *trans*-$[Os\{o\text{-}C_6F_4(PPh_2)_2\}_2Br_2]BF_4$ showed only an anomalously small positive shift. Interestingly the potentials observed for the analogous alkyldiphosphine iron complexes[18] were very similar to those recorded here, whereas one might have expected the 5d complexes to be less oxidising than the 3d. We also note that no ruthenium(IV) analogues have been obtained.[25] For the few examples where redox potentials have been recorded previously[25] the results agree, except for those complexes with the ligand *o*-$C_6H_4(PMe_2)_2$. Warren and Bennett[25] reported that the complex *trans*-$[Os\{o\text{-}C_6H_4(PMe_2)_2\}_2Cl_2]ClO_4$ gave a reversible $Os^{III}$–$Os^{IV}$ couple only at low temperatures (−30 °C), whereas it was found in this study that a reversible $Os^{III}$–$Os^{IV}$ couple was observed at room temperature. The stability of *trans*-$[Os\{o\text{-}C_6H_4(PMe_2)_2\}_2Cl_2]^{2+}$ is clearly demonstrated by the isolation of the solid osmium(IV) complex as a perchlorate salt.

*Osmium*(IV) *Complexes*.—Based on the electrochemical studies, which showed that all the complexes of $Os^{III}$ underwent reversible oxidation to $Os^{IV}$, chemical oxidation and isolation of the osmium(IV) complexes was attempted. The complexes of the alkyl-substituted ligands were readily generated in solution by dissolution of the complexes of $Os^{III}$ in concentrated $HNO_3$ at 0 °C, but dilution of these solutions with water, or even addition of the most concentrated solution available of $HBF_4$ (*ca.* 50% concentration), caused immediate regeneration of $Os^{III}$. The complexes *trans*-$[Os(L\text{–}L)_2X_2][ClO_4]_2$ [L–L = *o*-$C_6H_4(AsMe_2)_2$, *o*-$C_6H_4(AsMe_2)(PMe_2)$ or *o*-$C_6H_4(PMe_2)_2$] were precipitated successfully by addition of 70% $HClO_4$ at 0 °C. In contrast to a previous report[25] that the osmium(IV) complexes of *o*-$C_6H_4(PMe_2)_2$ are too unstable to isolate, we find that the dark green chloride and green-black bromide are relatively stable in the solid state and can be kept <0 °C for several days without detectable decomposition, and their solutions in $CF_3CO_2H$ show little decomposition in sealed cells in 24 h. Attempts to isolate osmium(IV) complexes of $Me_2PCH_2CH_2PMe_2$ failed, since although formed readily in solution (Table 5) they proved too soluble to precipitate even as $ClO_4^-$ salts, whilst conversely the $[Os\{o\text{-}C_6F_4(AsMe_2)_2\}_2X_2]BF_4$ complexes were poorly soluble in concentrated $HNO_3$ and only incompletely oxidised in suspension. Very similar results were obtained in the corresponding iron(III)–iron(IV) systems.[23] However in contrast to the iron complexes, the *trans*-$[Os(L\text{–}L)_2X_2]BF_4$ [L–L = $Ph_2PCH_2CH_2PPh_2$ or *o*-$C_6H_4(PPh_2)_2$] show electrochemically reversible $M^{III}$–$M^{IV}$ couples, and the osmium(III) complexes darken when suspended in concentrated $HNO_3$. The UV/VIS spectra obtained after dissolution of these solids in $CF_3CO_2H$ showed oxidation was incomplete, and pure osmium(IV) complexes were not obtained. All the complexes of $Os^{IV}$ decomposed immediately in most organic solvents with the exception of $CF_3CO_2H$.

**Table 5** Selected spectroscopic data for the osmium(IV) species

| Compound or ion | Colour | $E_{max}{}^a/10^3$ cm$^{-1}$ ($\varepsilon$/dm$^3$ mol$^{-1}$ cm$^{-1}$) |
|---|---|---|
| $[Os\{o\text{-}C_6H_4(PMe_2)_2\}_2Cl_2][ClO_4]_2$ | Dark green | 13.9 (250), 15.0 (380), 20.6 (sh) (220), 23.2 (sh) (280), 29.6 (1590) |
| $[Os\{o\text{-}C_6H_4(PMe_2)_2\}_2Br_2][ClO_4]_2$ | Green-black | 13.4 (sh) (2040), 14.3 (2856), 14.9 (sh) (2700), 24.9 (4590), 27.6 (sh) (2350) |
| $[Os\{o\text{-}C_6H_4(AsMe_2)(PMe_2)\}_2Cl_2][ClO_4]_2$ | Blue-black | 13.7 (900), 15.7 (1380), 18.7 (sh) (530), 25.6 (sh) (1050), 30.0 (4470) |
| $[Os\{o\text{-}C_6H_4(AsMe_2)(PMe_2)\}_2Br_2][ClO_4]_2$ | Green-black | 13.2 (sh) (1940), 14.4 (2815), 16.5 (sh), 19.5 (400), 25.4 (4410) |
| $[Os\{o\text{-}C_6H_4(AsMe_2)_2\}_2Cl_2][ClO_4]_2$ | Blue-black | 13.7 (650), 15.7 (1070), 19.7 (sh) (215), 29.8 (2470) |
| $[Os\{o\text{-}C_6H_4(AsMe_2)_2\}_2Br_2][ClO_4]_2$ | Green-black | 13.1 (sh) (1340), 14.3 (2040), 19.8 (310), 25.5 (10 480), 27.7 (sh) |
| $[Os\{o\text{-}C_6F_4(AsMe_2)_2\}_2Cl_2]^{2+\,b}$ | Dark blue | 14.6, 16.3, 18.9, 21.5, 29.7 |
| $[Os\{o\text{-}C_6F_4(AsMe_2)_2\}_2Br_2]^{2+\,b}$ | Dark green | 14.7, 15.9 (sh), 20.8, 24.9, 27.8 (sh) |
| $[Os(Me_2PCH_2CH_2PMe_2)_2Cl_2]^{2+\,b}$ | Green | 13.7, 15.2, 29.7 |
| $[Os(Me_2PCH_2CH_2PMe_2)_2Br_2]^{2+\,b}$ | Dark green | 13.4, 14.5, 24.7 |

[a] Freshly prepared solution in $CF_3CO_2H$. [b] Generated *in situ* in $CF_3CO_2H$ by $HNO_3$ oxidation of osmium(III) analogue (see text). Major bands only.

**Table 6** Refined EXAFS parameters for $[Os\{o\text{-}C_6H_4(AsMe_2)_2\}_2X_2]^{n+}$ (X = Cl or Br, $n$ = 0–2)[a]

| Complex | $d$(Os–X)$^b$/Å | $2\sigma^{2\,c}$/Å$^2$ | $d$(Os–As)$^b$/Å | $2\sigma^{2\,c}$/Å$^2$ | $E^c$/eV | F.i.$^d$ | $R^e$ |
|---|---|---|---|---|---|---|---|
| $[Os\{o\text{-}C_6H_4(AsMe_2)_2\}_2Cl_2]$ | 2.41(1) | 0.008(3) | 2.404(3) | 0.0059(6) | 10(1) | 4.9 | 23.7 |
| $[Os\{o\text{-}C_6H_4(AsMe_2)_2\}_2Cl_2]^+$ | 2.349(7) | 0.006(3) | 2.460(4) | 0.0068(7) | 11(2) | 7.5 | 22.0 |
| $[Os\{o\text{-}C_6H_4(AsMe_2)_2\}_2Cl_2]^{2+}$ | 2.278(6) | 0.0068(7) | 2.512(3) | 0.0083(2) | 5.9(8) | 3.5 | 19.5 |
| $[Os\{o\text{-}C_6H_4(AsMe_2)_2\}_2Br_2]$ | 2.577(6) | 0.0089(9) | 2.407(4) | 0.0069(3) | 14(2) | 7.3 | 27.2 |
|  | 2.548(3)$^f$ | 0.0077(2) |  |  |  |  |  |
| $[Os\{o\text{-}C_6H_4(AsMe_2)_2\}_2Br_2]^+$ | 2.515(8) | 0.003(1) | 2.443(4) | 0.0044(8) | 10.4(9) | 4.6 | 17.3 |
|  | 2.485(4)$^f$ | 0.0071(3) |  |  |  |  |  |
| $[Os\{o\text{-}C_6H_4(AsMe_2)_2\}_2Br_2]^{2+}$ | 2.400(4) | 0.0032(4) | 2.517(3) | 0.0050(3) | 7.3(8) | 3.1 | 16.6 |
|  | 2.384(5)$^f$ | 0.0084(3) |  |  |  |  |  |

[a] Standard deviations in parentheses; osmium $L_{III}$-edge data except where otherwise specified. [b] Errors arising from data collection and analysis are estimated to be ±0.02–0.03 Å in well defined co-ordination shells.[26] [c] Debye–Waller factor. [d] Fit index = $\Sigma_i[(\chi^T - \chi^E)k_i{}^3]^2$. [e] $R = [\int(\chi^T - \chi^E)k^3dk/\int\chi^Ek^3dk] \times 100\%$. [f] Bromine K-edge data.

The UV/VIS spectra of the osmium(IV) complexes were obtained in $CF_3CO_2H$ solutions, repetitive scanning showing no decomposition over *ca.* 1 h. The main features are listed in Table 5 and examples are in Fig. 3. Previous studies[5] of the magnetic properties ($\mu$ *ca.* 1.2) are consistent with a low-spin $t_{2g}{}^4$ ground state. The spectra are characterised by very broad absorptions, and an assignment of the major bands follows from that discussed above for the osmium(III) precursors. The two very broad overlapping features at *ca.* 13 000–16 000 cm$^{-1}$ are $\sigma$(P,As)⟶e(Os), which are shifted *ca.* 3000 cm$^{-1}$ to low energy from the counterparts in the osmium(III) spectra. The strong features in the range 24 000–29 000 cm$^{-1}$ are tentatively assigned as $\sigma$(P,As)⟶$a_1$(Os) and probably coincide with the $\pi$(X)⟶e(Os) transitions. Support for the latter proposal comes from the spectrum of $[Os\{o\text{-}C_6H_4(PMe_2)_2\}_2Br_2][ClO_4]_2$, which showed a distinct shoulder at 27 600 cm$^{-1}$ tentatively assigned as the $\pi$(Br)⟶e(Os) c.t. band. The small shift in the energy of the $\sigma$(P,As)⟶$a_1$(Os) band between $Os^{III}$ and $Os^{IV}$ could be due to the increased energy of the $d_{z^2}$ orbital as the Os–X bond shortens upon oxidation.

*EXAFS Studies.*—Osmium $L_{III}$-edge and bromine K-edge EXAFS data were recorded for the series of diarsine complexes *trans*-$[Os\{o\text{-}C_6H_4(AsMe_2)_2\}_2X_2]^{n+}$ (X = Cl or Br, $n$ = 0–2). The spectra analysed satisfactorily and the refined data are presented in Table 6 with typical background-subtracted $k^3$-weighted EXAFS and Fourier transforms shown in Fig. 4.

Phase-shift reliability was checked by analysis of data from the model compound, *trans*-$[Os\{o\text{-}C_6H_4(AsMe_2)_2\}_2Cl_2]ClO_4$. Good agreement with the crystallographic data was obtained (see below) and so analysis proceeded using calculated phase shifts and back-scattering factors without further modification. It should be noted that the rather large $R$ factors and fit indices are a result of the presence in each of the osmium $L_{III}$-edge spectra of a shell at *ca.* 4.8 Å which probably arises from a number of osmium to ligand carbon distances. It was not possible to model these interactions satisfactorily and their effects are seen at low $k$ in the background-subtracted EXAFS spectrum. Fourier filtering ($r$ = 0–3.5 Å) the data resulted in $R$ factors of 14–16%. Bromine K-edge EXAFS was used to confirm the validity of Os–Br distances found from the osmium $L_{III}$-edge data. Single-shell fits on Fourier-filtered data are quoted in Table 6 and agree within experimental error. A diffuse shell at *ca.* 3.5 Å due to scattering from the four arsenic atoms and one at twice the Br–Os distance (4.8–5.15 Å) due to the *trans*-bromine were also observed in each case, but the data quality was not sufficient to justify a full fit of these further shells.

The bond lengths obtained are consistent with those from related compounds in appropriate oxidation states which have been crystallographically characterised. Osmium(II)–halide and -arsenic distances are best exemplified by the complexes *trans*-$[Os\{(Ph_2P)_2C{=}CH_2\}_2Cl_2]$,[27] and $[Os\{o\text{-}C_6H_4(AsMe_2)_2\}_2Br_2(CO)]$[28] which has one mono- and one bi-dentate diarsine ligand. The Os–Cl distance in the former is 2.431 Å whilst the average Os–Br (*trans* Br) and Os–As (*trans* As) distances in the latter are 2.57 and 2.44 Å respectively. The $Os^{III}$–As and $Os^{III}$–Cl distances have been noted in the X-ray structure reported above, whilst a typical $Os^{III}$–Br (*trans* Br) distance is seen in *mer*-$[Os(PPh_3)_2(NCMe)Br_3]$ at 2.49 (average) Å.[29] Finally, interactions of $Os^{IV}$ with bromide and arsenic are observed in $[Os(AsPh_3)_2Br_4]$ with $d(Os^{IV}\text{–}As)$ = 2.569 Å and $d(Os^{IV}\text{–}Br)$ = 2.46 (average) Å.[30]

Inspection of the bond-length data obtained from EXAFS analysis reveals opposite trends in the Os–As and Os–X bond lengths, the former increasing with the metal oxidation state, the latter decreasing. It has been noted previously[4] that osmium to halogen distances tend to decrease with increasing metal oxidation state and this may be attributed to the increased electrostatic attraction as the metal nucleus becomes formally more positively charged, resulting in bond-length contraction. The trend of increasing osmium to arsenic bond distances may

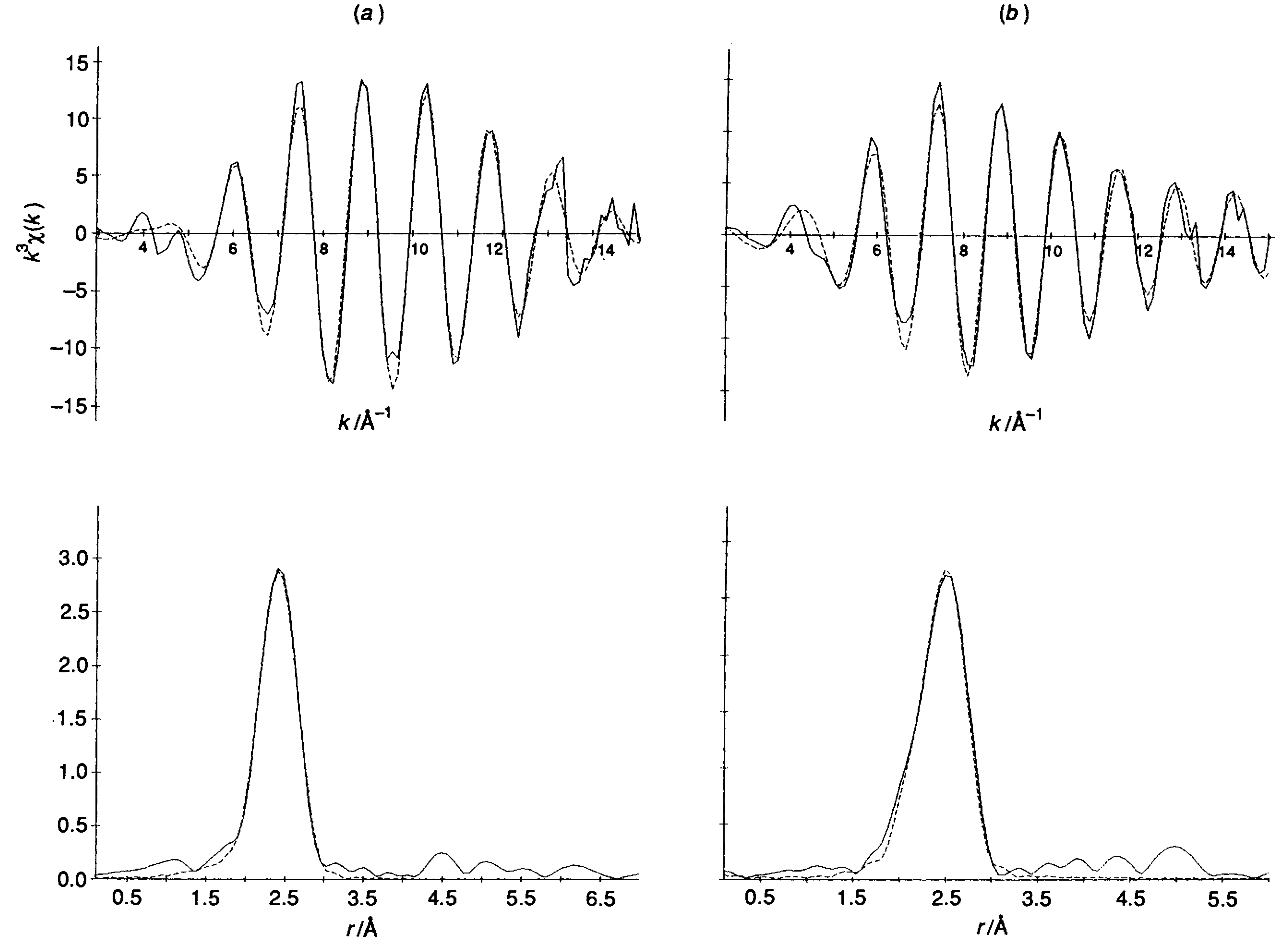

**Fig. 4** Background-subtracted osmium $L_{III}$-edge EXAFS [$k^3$ weighted; experimental (——), theory (– – –)] and Fourier transform [below; experimental (——), theory (– – –)] for (*a*) *trans*-[Os{*o*-$C_6H_4(AsMe_2)_2$}$_2Cl_2$][$ClO_4$]$_2$ and (*b*) *trans*-[Os{*o*-$C_6H_4(AsMe_2)_2$}$_2Br_2$][$ClO_4$]$_2$

be rationalised in terms of a progressively weaker interaction of the soft arsenic donor atoms with the increasingly hard *trans*-$OsX_2^{n+}$ unit as *n* increases from 0 to 2. In addition, as the metal oxidation state increases its radius decreases with the result that steric effects are also a factor. Since the arsine ligands are most sterically demanding but less strongly bonded they are more affected than the halide ligands.

## Acknowledgements

We thank the SERC and BP Chemicals for support, Professor M. B. Hursthouse for the X-ray data collection by the SERC service, S. K. Harbron and L. Rayson for preliminary studies, and the Director of the Daresbury Laboratory for the provision of facilities.

## References

1 Part 39, W. Levason, M. D. Spicer and M. Webster, *Inorg. Chem.*, in the press.
2 R. A. Cipriano, W. Levason, R. A. S. Mould, D. Pletcher and M. Webster, *J. Chem. Soc., Dalton Trans.*, 1990, 339.
3 R. A. Cipriano, W. Levason, R. A. S. Mould, D. Pletcher and M. Webster, *J. Chem. Soc., Dalton Trans.*, 1990, 2609.
4 N. R. Champness, W. Levason, R. A. S. Mould, D. Pletcher and M. Webster, *J. Chem. Soc., Dalton Trans.*, 1991, 2777.
5 R. S. Nyholm and G. J. Sutton, *J. Chem. Soc.*, 1958, 572.
6 J. Chatt and R. G. Hayter, *J. Chem. Soc.*, 1961, 896.
7 B. P. Sullivan and T. J. Meyer, *Inorg. Chem.*, 1982, **21**, 1037.
8 A. Mezzetti, A. Del Zotto and P. Rigo, *J. Chem. Soc., Dalton Trans.*, 1990, 2515.
9 A. R. Chakravarty, F. A. Cotton and W. Schwotzer, *Inorg. Chim. Acta*, 1984, **84**, 179.
10 M. R. Snow and E. R. T. Tiekink, *Acta Crystallogr., Sect. B*, 1988, **44**, 676.
11 G. M. Sheldrick, SHELX 76, Program for crystal structure determination, University of Cambridge, 1976.
12 *International Tables for X-Ray Crystallography*, Kynoch Press, Birmingham, 1974, vol. 4, pp. 99, 149.
13 P. Roberts and G. M. Sheldrick, XANADU, Program for crystallographic calculations, University of Cambridge, 1979.
14 C. K. Johnson, ORTEP II, Report ORNL-5138, Oak Ridge National Laboratory, TN, 1976.
15 N. Binsted, PAXAS, Program for the Analysis of X-ray Absorption Spectra, University of Southampton, 1988.
16 N. Binsted, S. J. Gurman and J. W. Campbell, EXCURVE 90, SERC Daresbury Laboratory Program, Daresbury Laboratory, Warrington, 1990.
17 J. M. Corker, J. Evans, W. Levason, M. D. Spicer and P. Andrews, *Inorg. Chem.*, 1991, **30**, 331.
18 J. I. Zink, P.-O. Liu and B. Anfield, *Inorg. Chem.*, 1979, **18**, 1013.
19 C.-M. Che, W.-K. Cheng, T.-F. Lai, C.-W. Poon and T. C. W. Mak, *Inorg. Chem.*, 1987, **26**, 1678.
20 J. D. Buhr, J. R. Winkler and H. Taube, *Inorg. Chem.*, 1980, **19**, 2416.
21 L. R. Gray, D. J. Gulliver, W. Levason and M. Webster, *J. Chem. Soc., Dalton Trans.*, 1983, 133.
22 P. Kreisman, G. A. Rodley, R. Marsh and H. B. Gray, *Inorg. Chem.*, 1972, **11**, 3040.
23 S. K. Harbron, S. J. Higgins, W. Levason, M. C. Feiters and A. T. Steel, *Inorg. Chem.*, 1986, **25**, 1789.
24 L. R. Hanton, J. Evans, W. Levason, R. J. Perry and M. Webster, *J. Chem. Soc., Dalton Trans.*, 1991, 2039.
25 L. F. Warren and M. A. Bennett, *Inorg. Chem.*, 1976, **15**, 3126.

26 J. M. Corker, J. Evans, H. Leach and W. Levason, *J. Chem. Soc., Chem. Commun.*, 1989, 181.

27 F. A. Cotton, M. P. Diebold and M. Matusz, *Polyhedron*, 1987, **6**, 1131.

28 F. Bottomley, I. J. B. Lin and P. S. White, *J. Chem. Soc., Dalton Trans.*, 1978, 1726.

29 F. A. Cotton, S. A. Duraj, C. C. Hinckley, M. Matusz and W. J. Roth, *Inorg. Chem.*, 1984, **23**, 3080.

30 C. C. Hinkley, M. Matusz and P. D. Robinson, *Acta Crystallogr., Sect. C*, 1988, **44**, 371.

*Received* 19*th February* 1992; *Paper* 2/00886F